

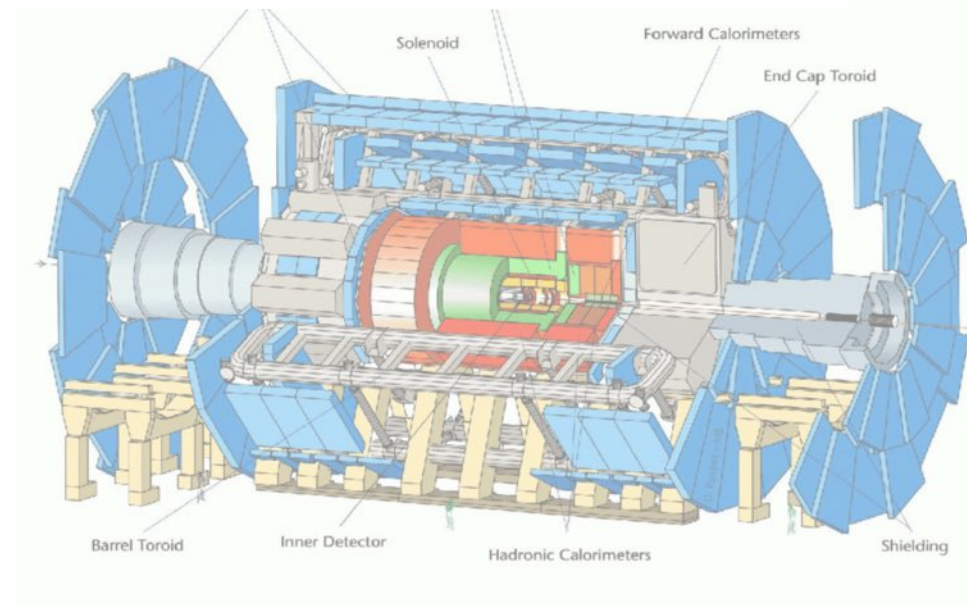
Search for physics beyond the Standard Model in the decays of neutral B mesons with ATLAS

Sandro Palestini (CERN)

On behalf of the ATLAS Collaboration

WIN2019

27th International Workshop on Weak
Interactions and Neutrinos



Content



The search for physics beyond the Standard Model represents a large sector of Flavor Physics:

- Processes are naturally suppressed in SM can be very sensitive to New Physics through virtual loops involving new particles / new carriers at very large mass scales.
- Quantum Mechanical oscillations allow the measurements of amplitudes and phases, assessing CP violation and providing accurate tests of the SM

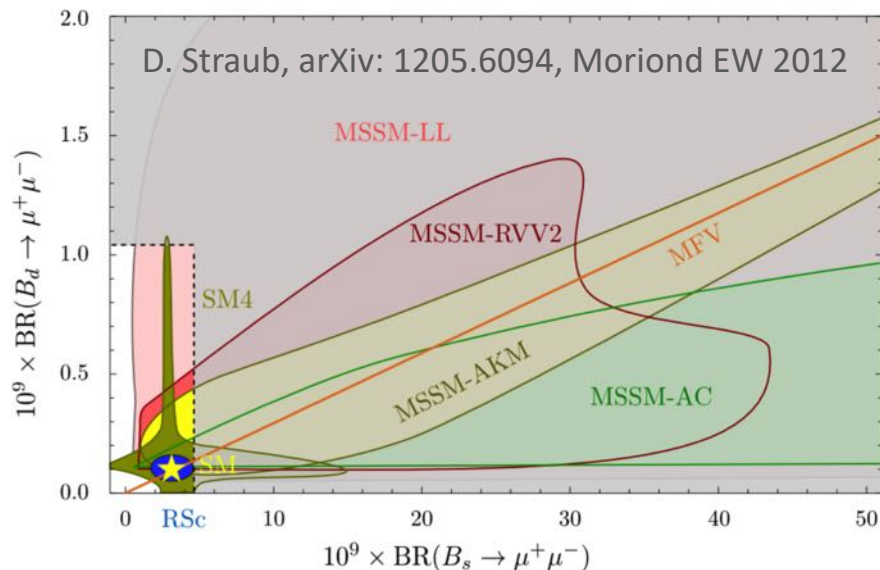
Two studies are discussed here:

- Rare decays of $B^0(d\bar{b}), B_s^0(s\bar{b})$ to $\mu^+\mu^-$ pairs: FCNC mediated process
Result recently published
- CP violation search in $B_s^0 \rightarrow J/\psi \phi$: weak phases in B_s^0 mixing and $b \rightarrow c\bar{c}s$ decay amplitude
Preliminary results, presented this spring

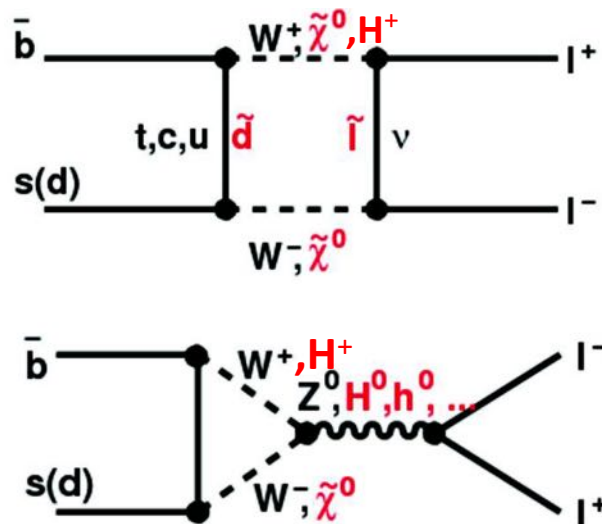
The rare decays
of B_S^0 and B^0 into $\mu^+\mu^-$ pairs

Motivation and available results

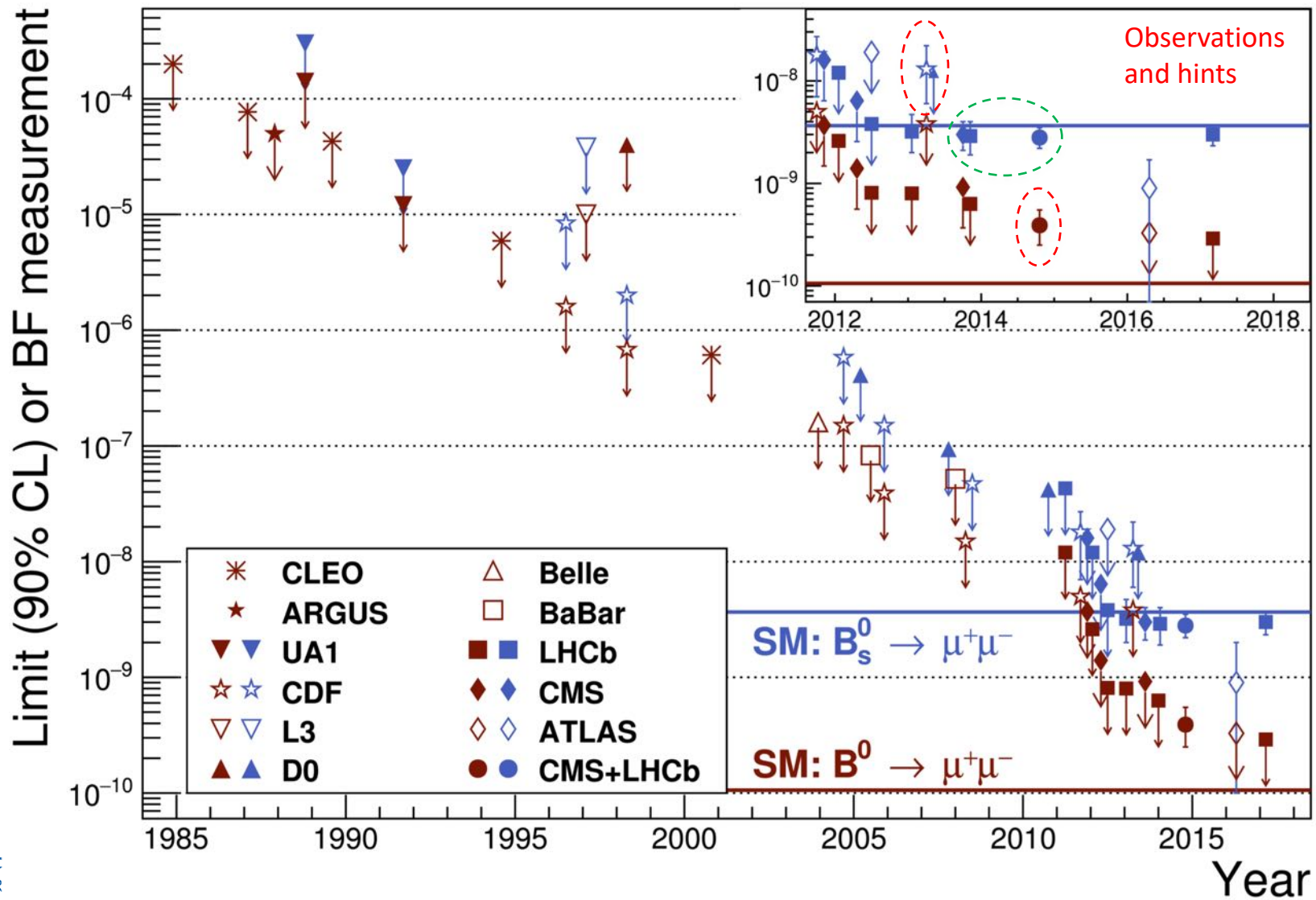
- FCNC process, further affected by helicity suppression, and predicted accurately in the SM:
 - $BR(B_s^0 \rightarrow \mu^+ \mu^-) = (3.65 \pm 0.23) \times 10^{-9}$,
 - $BR(B^0 \rightarrow \mu^+ \mu^-) = (1.06 \pm 0.09) \times 10^{-10}$ [C. Bobeth et al., PRL 112 (2104) 101801]
 - Sensitive to physics beyond SM



Examples of diagrams with BSM contributions



The long lasting search for the decay to muon pairs



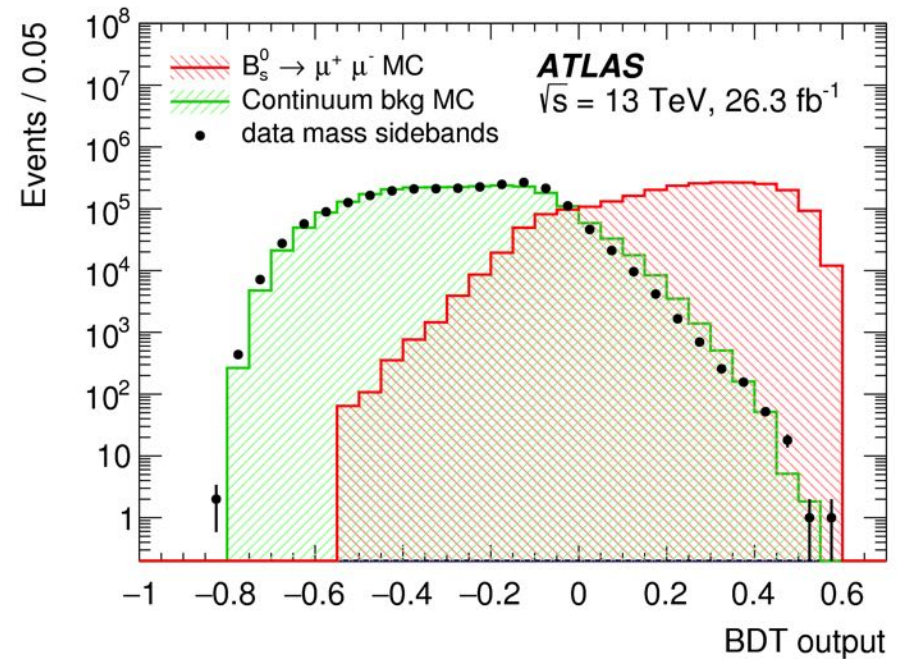
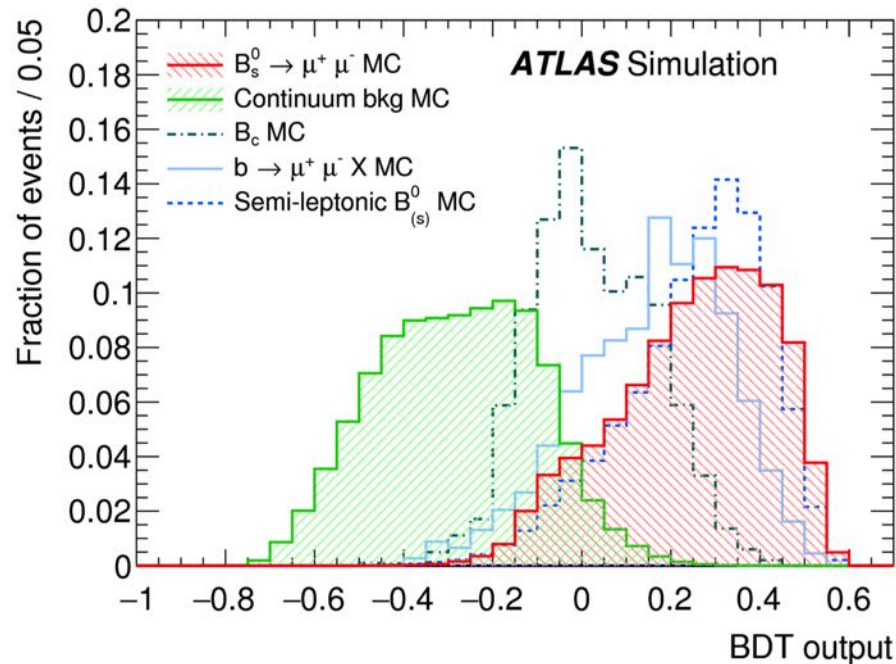
Analysis flow



- **Trigger: muon pairs:** $p_T(\mu) > 4 \text{ GeV}$ or 6 GeV , **Selection:** $p_T(B) > 8 \text{ GeV}$, $|\eta(B)| < 2.5$
- Require track reconstruction in both the inner detector and the muon spectrometer (*combined muons*)
- Reconstruct signal $B_{(s)}^0 \rightarrow \mu^+ \mu^-$
and **reference channels:** $B^+ \rightarrow J/\psi K^+$, $B_{(s)}^0 \rightarrow J/\psi \phi$ ($J/\psi \rightarrow \mu^+ \mu^-$, $\phi \rightarrow K^+ K^-$), used for normalisation and calibration
- $m(\mu^+ \mu^-)$ mass range (blinded) for signal 5166-5526 MeV, wider for background studies: 4766 to 5966 MeV ,
- Background:
 - **Combinatorial background:** dominant component, small mass dependence
 - **Partially reconstructed $B \rightarrow \mu \mu X$ decays:** low mass, the tail extends barely to the signal region
 - **Peaking background** from double-hadrons misidentification in $B_{(s)}^0 \rightarrow hh'$ (smaller component, but overlaid with signal)

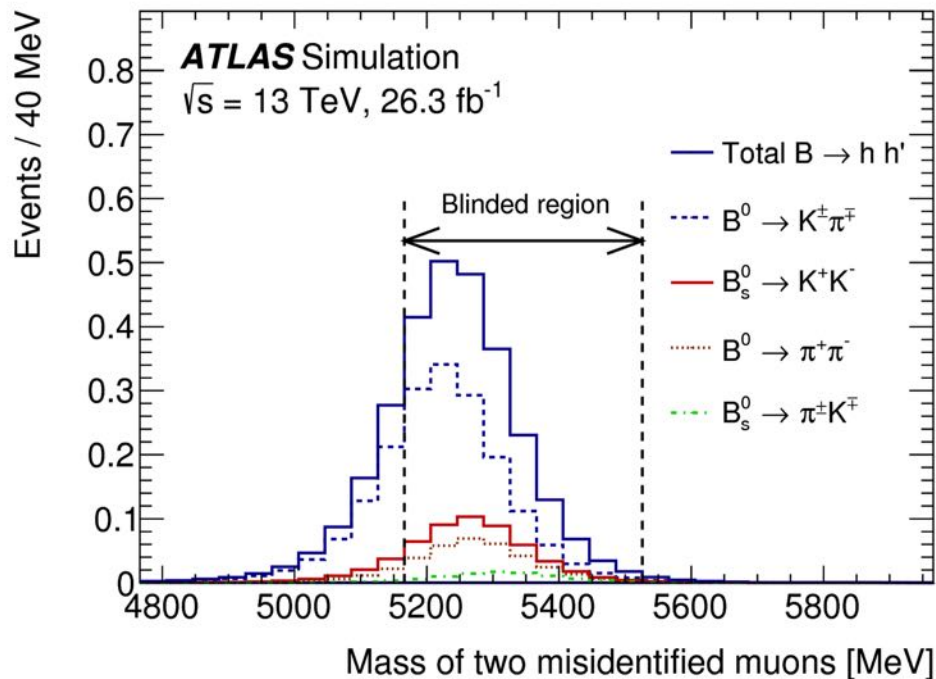
Classifier for *continuum* background

- Enhance signal to background ratio by means of:
 - MVA classifier** against continuum background, exploiting signal characteristics (secondary vertex, collinearity etc.) against dominating backgrounds (muons from different B decay, background tracks form same primary interaction and from pile-up).



Peaking background

- Enhance signal to background ratio by means of:
 2. Dedicated selection against **fake muons**: compare momentum measurements in Inner Detector and Muon Spectrometer and quality requirements on track
 - Low punch-through rates : background is mainly due to kaon and pion decays in flight (two body, forward). Misidentification rate at $\leq 0.1\%$ after optimized selection.



Particle misidentification creates a background under the B^0 signal: 0.1% rejection per-hadron is needed to bring this background well below the SM prediction for $B^0 \rightarrow \mu^+ \mu^-$

Normalization

The yield N_s , N_d of $B^0 \rightarrow \mu^+ \mu^-$, $B^0 \rightarrow \mu^+ \mu^-$ events is normalized to the channel:

$$B^+ \rightarrow J/\psi (\rightarrow \mu^+ \mu^-) K^+$$

using the equation:

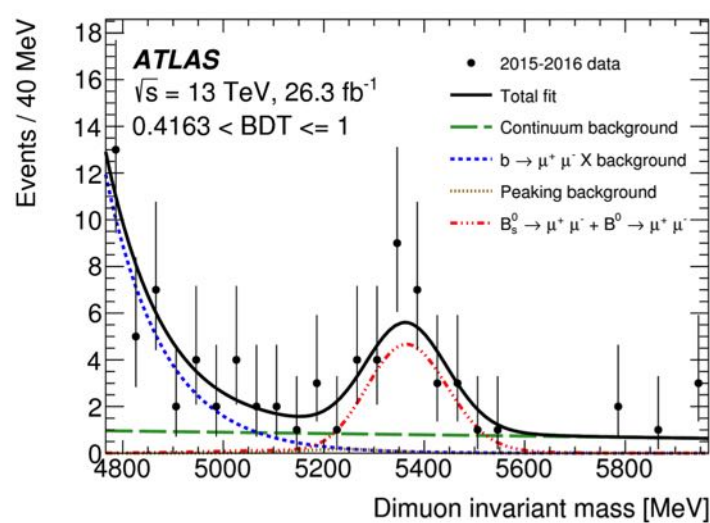
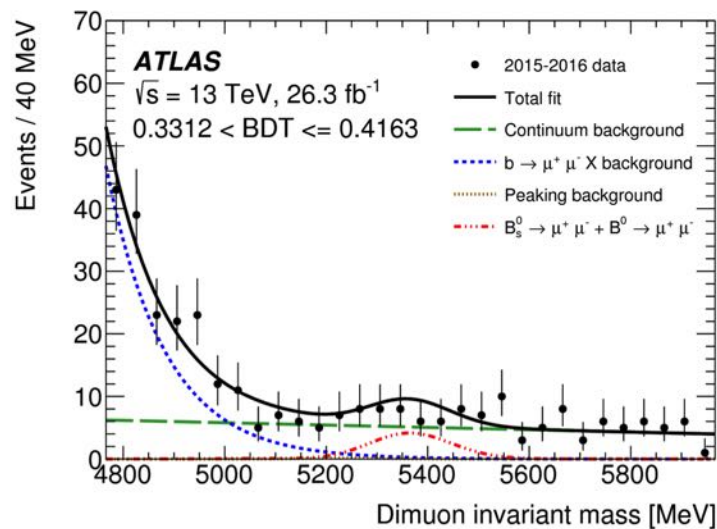
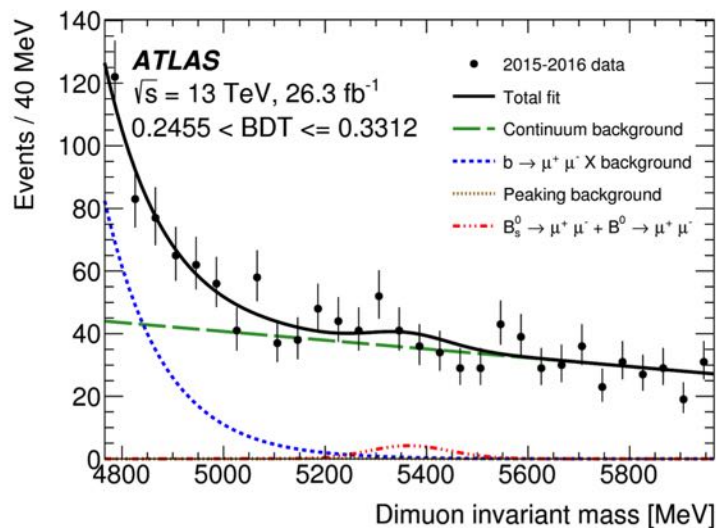
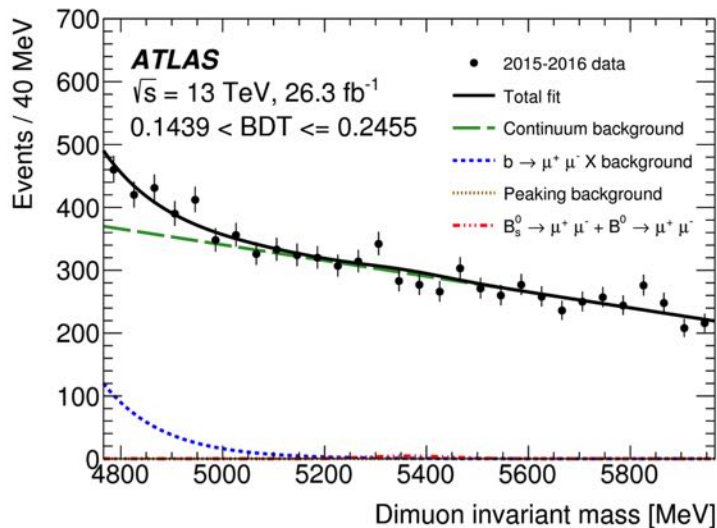
$$\mathcal{B}(B_{(s)}^0 \rightarrow \mu^+ \mu^-) = \frac{N_{d(s)}}{\varepsilon_{\mu^+ \mu^-}} \times [\mathcal{B}(B^+ \rightarrow J/\psi K^+) \times \mathcal{B}(J/\psi \rightarrow \mu^+ \mu^-)] \frac{\varepsilon_{J/\psi K^+}}{N_{J/\psi K^+}} \times \frac{f_u}{f_{d(s)}}$$

Systematic uncertainties enter in the fit model ($N_{d(s)}$, $N_{J/\psi K^+}$), in the efficiency ratio, and in the external inputs (BRs and production ratio).

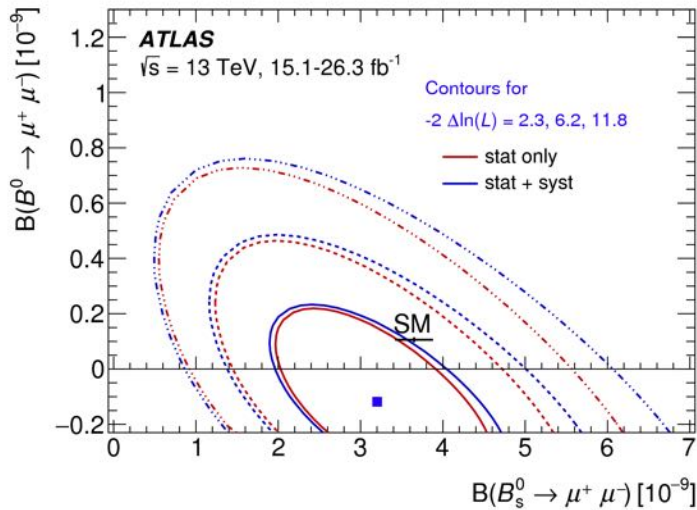
The statistical uncertainty largely dominates.

Signal extraction with likelihood fit over mass distribution, in different intervals of continuum-BDT output.

Muon pair invariant mass in four interval of BDT output



Likelihood contour for simultaneous fit

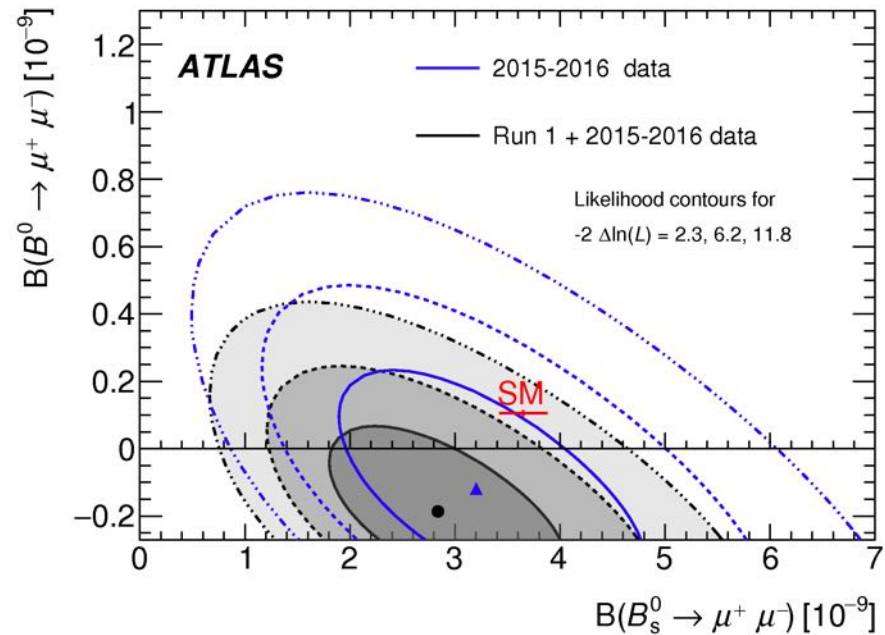


Run-2 2015/2016 results:

$$\mathcal{B}(B_s^0 \rightarrow \mu^+ \mu^-) = (3.21^{+0.90+0.48}_{-0.83-0.31}) \times 10^{-9}$$

$$\mathcal{B}(B^0 \rightarrow \mu^+ \mu^-) = (-1.3^{+2.2+0.7}_{-1.9-0.8}) \times 10^{-10}$$

ATLAS, JHEP 04 (2019) 098 (arXiv:1812.03017)



Combined ATLAS results:

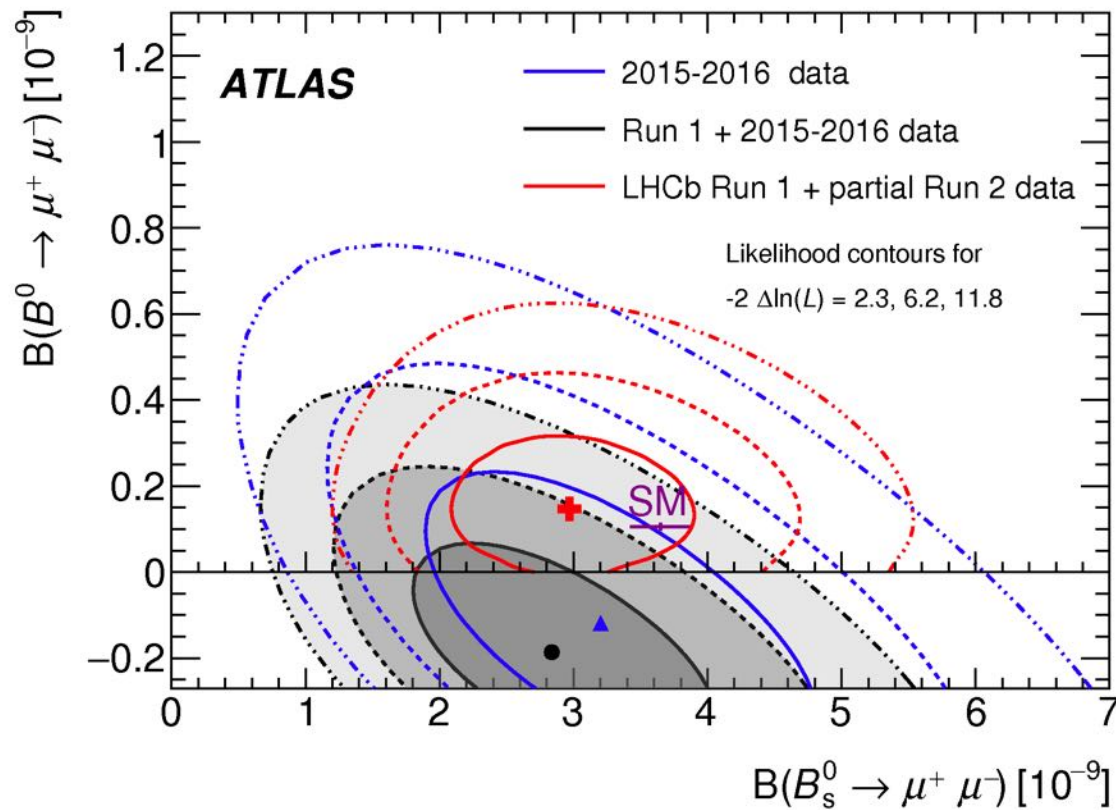
$$\mathcal{B}(B_s^0 \rightarrow \mu^+ \mu^-) = (2.8^{+0.8}_{-0.7}) \times 10^{-9}$$

$$\mathcal{B}(B^0 \rightarrow \mu^+ \mu^-) = (-1.9 \pm 1.6) \times 10^{-10}$$

$$< 2.1 \times 10^{-10} \text{ at 95\% CL}$$

Compatible with Standard Model prediction at 2.4 sigma

Comparison with LHCb



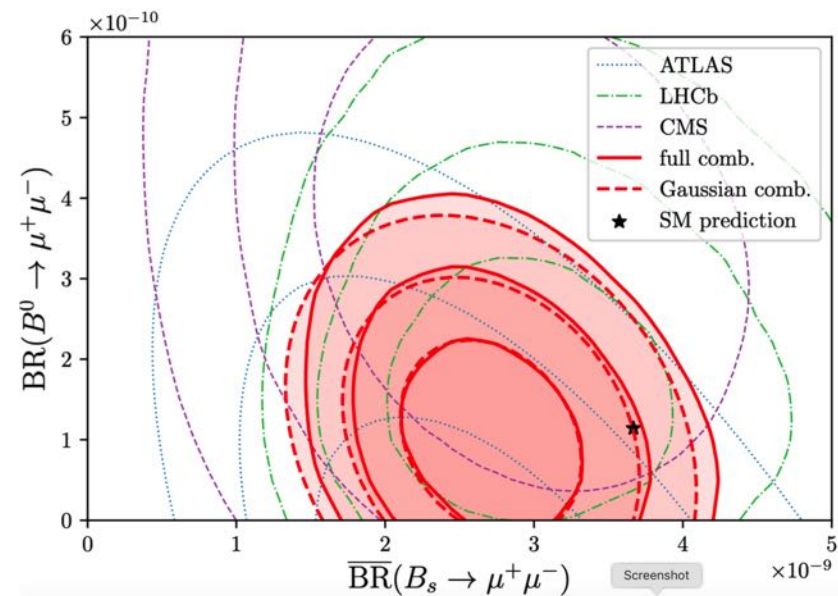
Also well compatible with LHCb results.

Phys. Rev. Lett. 118 (2017) 191801
(arXiv:1703.05747)

Official combination of results not available yet.

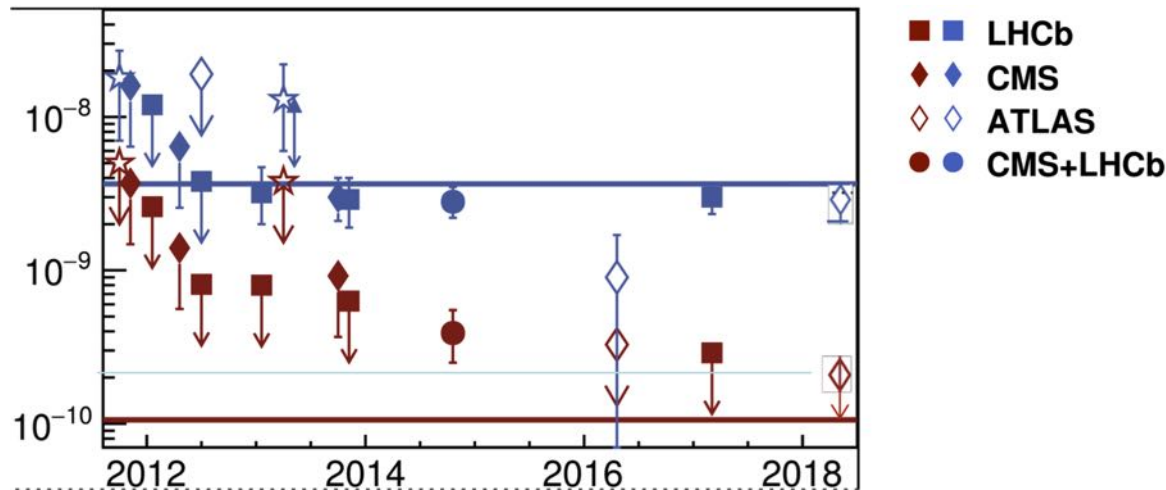
Unofficial ones (e.g. David Straub, Moriond EW 2019) remarked a combined 2 sigma deviation on $BR(B^0_s)$, with some impact to fits of coefficients in effective field theories.

$BR(B^0)$ appears well in line with SM prediction, but is not measured yet.



J. Aebischer, W. Altmannshofer, D. Guadagnoli, M. Reboud, P Stangl and M. Straub, arXiv:1903.10434

Conclusions on rare decays



- Vast improvement with LHC data
- BR(Bs) now measured at about 10% uncertainty
- Not there yet with BR(B0)
 - Standard Model is still confirmed
- Further increase in sensitivity with full Run-2 and High Luminosity LHC:
 - Statistical errors reduced by factor 2 and 6 respectively
 - Theoretical uncertainty might enter the game in the future
 - Already attempting to add the lifetime to the comparison: SM predicts the decay for B_s to occur through the B_{s,H} state (longer lifetime): need some % lifetime accuracy to test.

Determination of φ_s and $\Delta\Gamma_s$
from the decay of B_S to $J/\psi \phi$

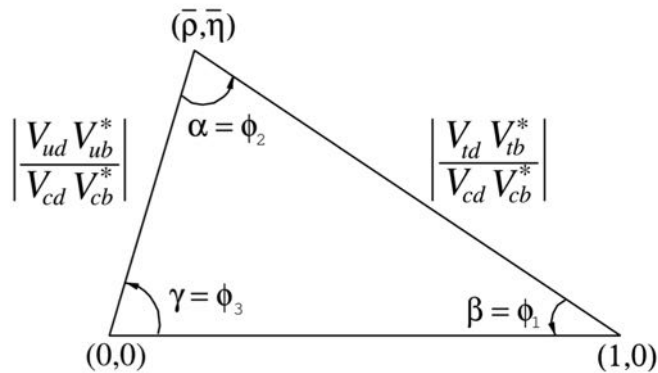
Quark mixing matrix

$$\frac{-g}{\sqrt{2}}(\bar{u}_L, \bar{c}_L, \bar{t}_L)\gamma^\mu W_\mu^+ V_{\text{CKM}} \begin{pmatrix} d_L \\ s_L \\ b_L \end{pmatrix} + \text{h.c.}, \quad V_{\text{CKM}} \equiv V_L^u V_L^{d\dagger} = \begin{pmatrix} V_{ud} & V_{us} & V_{ub} \\ V_{cd} & V_{cs} & V_{cb} \\ V_{td} & V_{ts} & V_{tb} \end{pmatrix}$$

$$V_{\text{CKM}} = \begin{pmatrix} 1 - \lambda^2/2 & \lambda & A\lambda^3(\rho - i\eta) \\ -\lambda & 1 - \lambda^2/2 & A\lambda^2 \\ A\lambda^3(1 - \rho - i\eta) & -A\lambda^2 & 1 \end{pmatrix} + \mathcal{O}(\lambda^4)$$

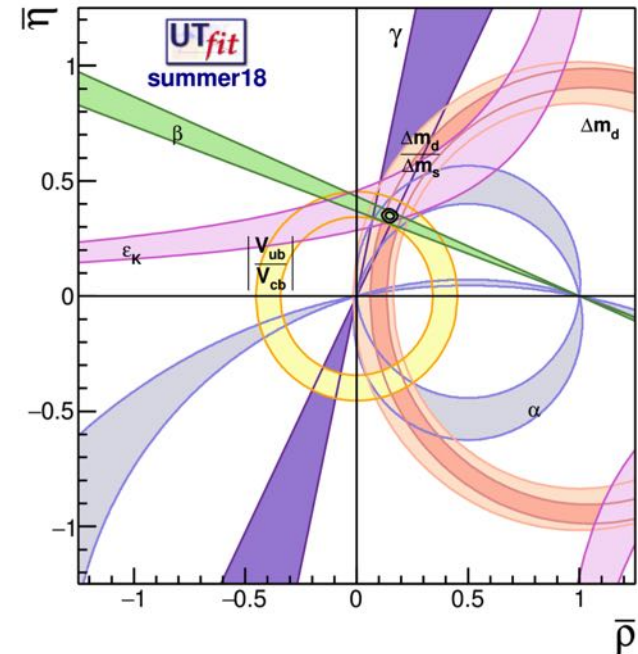
Wolfenstein, PDG:
 $\lambda = 0.22453 \pm 0.00044$, $A = 0.836 \pm 0.015$,
 $\bar{\rho} = 0.122^{+0.018}_{-0.017}$, $\bar{\eta} = 0.355^{+0.012}_{-0.011}$.

3 mixing angles (real rotations) and one phase in the unitary mixing angles. Unitarity (orthogonality) can be illustrated in triangular constructions, like the (db) one, studied in the B^0 system:



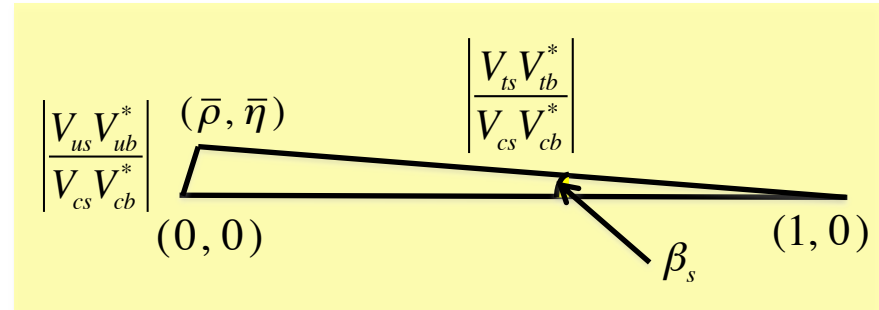
CP violation: $\eta \neq 0$.

New Physics: break of unitarity, deviations from predictions for amplitudes or phases



The B_s^0 case

- B_s^0 mixing has become more accessible with LHC, and a similar triangle can be drawn for the B_s^0 system - here (sb) :
- Here the parameters have different values:
- η and ρ have different values:
 $\eta_{sb} \sim \lambda^2 \eta_{db} \sim O(0.01)$
- The small predicted value makes the value of φ_s more sensitive to the NP.

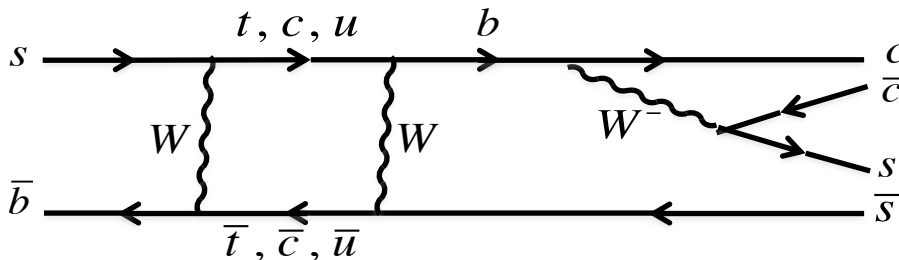


$$\beta_s = \arg[-(V_{ts}V_{tb}^*)/(V_{cs}V_{cb}^*)].$$

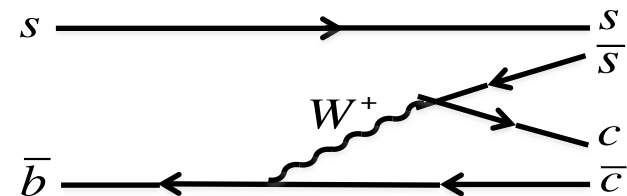
$$\varphi_s = -2\beta_s,$$

$$\text{SM: } \varphi_s = -0.0363 \pm 0.0016 \text{ rad}$$

The approach used is via a $(b \rightarrow c \bar{c} s)$ transition, namely in $B_s^0 \rightarrow J/\psi \phi$:



Decay amplitude with oscillation, weak phase $\cong 2 \times \arg(V_{ts}V_{tb}^*) + \arg(V_{cb}V_{cs}^*)$



Decay amplitude without oscillation, weak phase : $\arg(V_{cs}V_{cb}^*)$

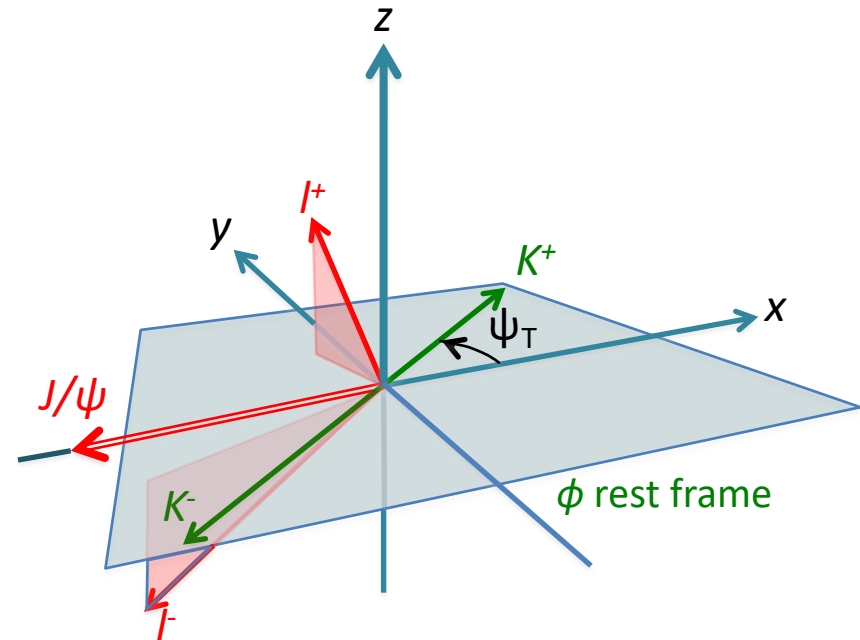
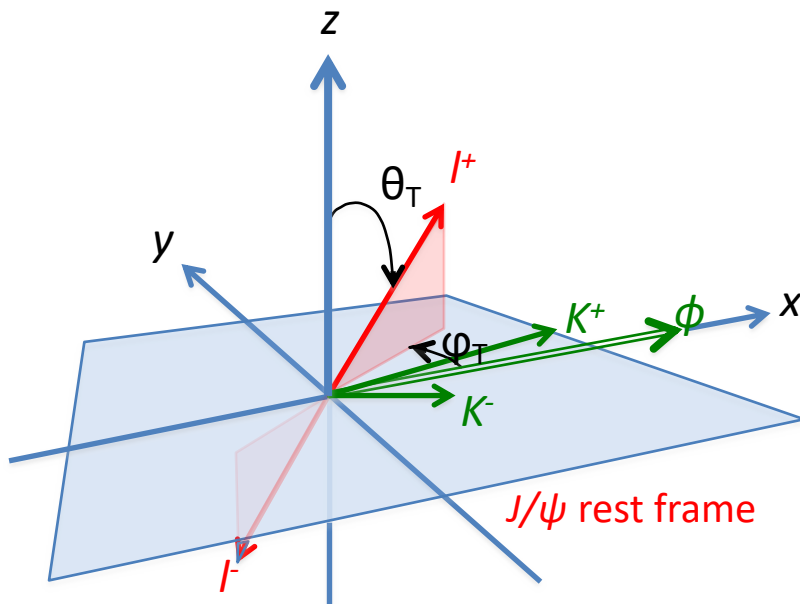
The B^0_s case - 2



- **Vector-Vector** final state: CP of final states depends of polarization, and must be determined but studying the **angular correlations in the final state**
 - *(added complexity compared to, e.g. $B^0 \rightarrow J/\psi K_S$)*
- **Lifetime difference**: the B_{SH} and B_{SL} eigenstates have different lifetime:
 - the two contributions and their interference term can be used to to extract φ_s from a time dependent study on the time scale of τ_s and $\Delta\tau_s$ (1.5, 0.15 ps)
 - *(This handle is not present in $B^0 \rightarrow J/\psi K_S$)*
- A better sensitivity is achieved by assessing the b / \bar{b} flavor at production
 - Need **flavor-tagging**, based on other observables in $p p$ scattering
 - Need **decay-time resolution** comparable to $1/\Delta m_s = 0.06$ ps
 - *(Comparable to CP and decay-time correlations in $e^+e^- \rightarrow B^0 \bar{B}^0$, with slower oscillations)*

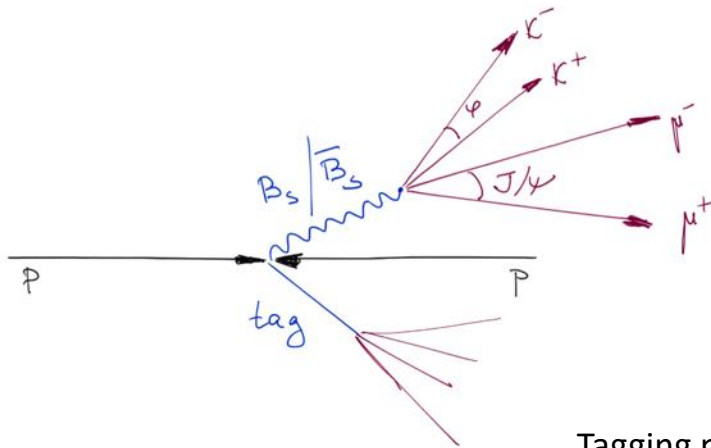
Angular variables

The “*transversity angles*” are used to describe the angular distributions:



In the J/ψ (or ϕ) rest frames, the **direction of ϕ** (opposite to J/ψ) defines the x axis, and the xy -plane is defined by the K^+K^- decay plane, with K^+ oriented towards positive y ; θ_T and ϕ_T are the polar angles of l^+ , ψ_T is the angle between K^+ and x -axis

Flavor tagging



Based observing a p_T weighted charge sum performed over cone centered on leptons and b-tagged jets.

Tagging is calibrated on a sample of $B^+ \rightarrow J/\psi K^+$

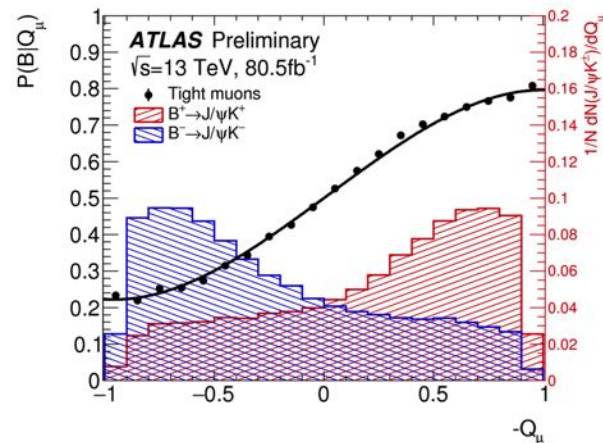
Tagging performance evaluated on B^+ sample

Tag method	Efficiency [%]	Effective Dilution [%]	Tagging Power [%]
Tight muon	4.50 ± 0.01	43.8 ± 0.2	0.862 ± 0.009
Electron	1.57 ± 0.01	41.8 ± 0.2	0.274 ± 0.004
Low- p_T muon	3.12 ± 0.01	29.9 ± 0.2	0.278 ± 0.006
Jet	5.54 ± 0.01	20.4 ± 0.1	0.231 ± 0.005
Total	14.74 ± 0.02	33.4 ± 0.1	1.65 ± 0.01

Effective dilution: $2 \times P(B/Q_x) - 1$

Tagging power: Efficiency \times Effective-dilution²

For comparison: LHCb's TP=4.7% , including same-side tagging
And equivalent quantity larger in e+e- ($B^0 B^0$ bar correlation)



Angular and time dependent amplitudes

$$\frac{d^4\Gamma}{dt d\Omega} = \sum_k \mathcal{O}^{(k)}(t) g^{(k)}(\theta_T, \psi_T, \varphi_T)$$

Full list provided below as additional material, here just a few terms shown at first order in φ_s :

10 terms corresponding to

- 3 square terms of defined transversity amplitudes
- 3 interference terms between transversity amplitudes
- 4 terms for the square of the K+K- non-resonant amplitude and the corresponding interference terms with the transversity amplitudes

$$(1) \cong |A_0|^2 \left[e^{-\Gamma_L t} \pm e^{-\Gamma_S t} \sin(\Delta m_s t) \times \varphi_s \times TP \times e^{-0.5(\sigma_t \Delta m_s)^2} \right] \times \\ \times 2 \cos^2 \psi_T (1 - \sin^2 \theta_T \cos^2 \phi_T)$$

$$(6) \cong |A_0| |A_\perp| \left[\frac{1}{2} (e^{-\Gamma_L t} - e^{-\Gamma_H t}) \cos \delta_{||} \times \varphi_s \pm e^{-\Gamma_S t} \cos(\delta_\perp - \Delta m_s t) \times TP \times e^{-0.5(\sigma_t \Delta m_s)^2} \right] \times \\ \times \frac{1}{\sqrt{2}} \sin 2\psi_T \sin^2 \theta_T \sin 2\phi_T$$

$$(9) \cong |A_S| |A_\perp| \sin(\delta_\perp - \delta_S) \left[e^{-\Gamma_H t} \mp e^{-\Gamma_S t} \sin(\Delta m_s t) \times \varphi_s \times TP \times e^{-0.5(\sigma_t \Delta m_s)^2} \right] \times \\ \times \frac{1}{3} \sqrt{6} \sin \psi_T \sin 2\theta_T \cos \phi_T$$

Angular and time dependent amplitudes

$$\frac{d^4\Gamma}{dt d\Omega} = \sum_k \mathcal{O}^{(k)}(t) g^{(k)}(\theta_T, \psi_T, \varphi_T)$$

- Note the strong phases present in the interference terms
- CP = ± 1 contributions enter with \pm in the fast oscillating term
- Amplitude and phase of non resonant K+K- contribution are extracted from the fit

$$TP = 1.65\% \quad e^{-0.5(\sigma_t \Delta m_s)^2} \cong 0.47$$

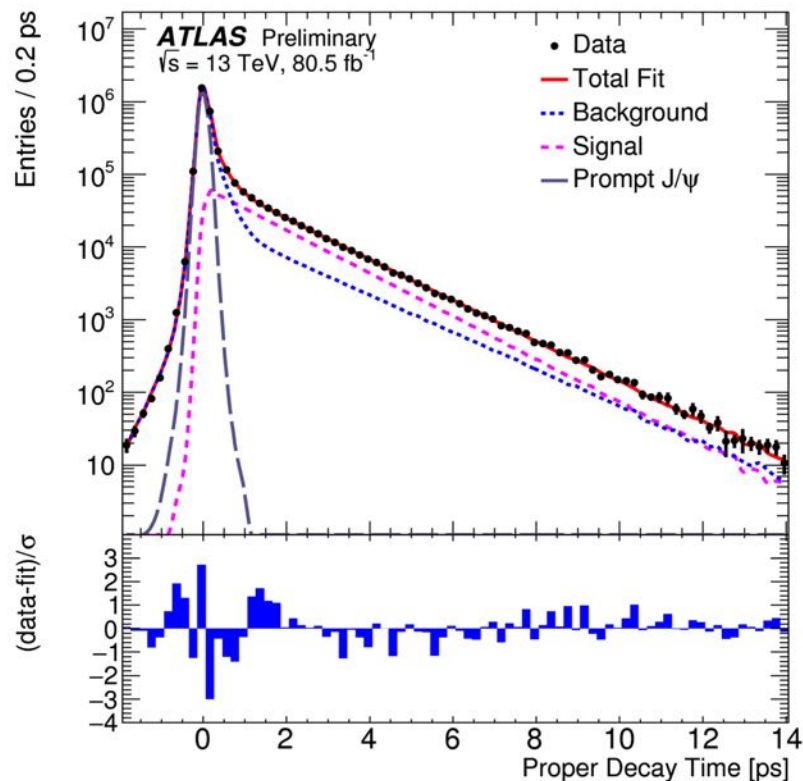
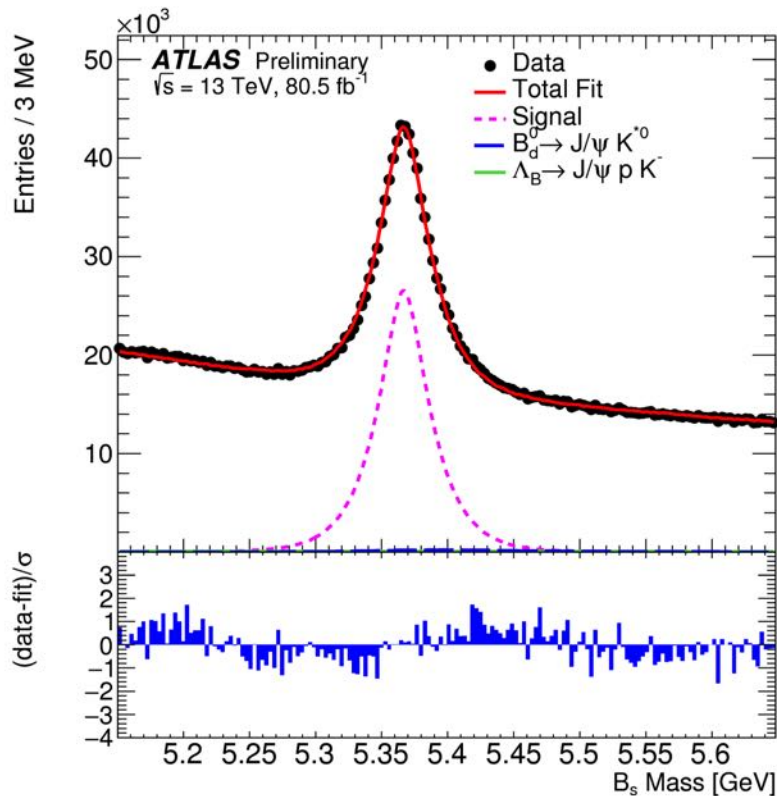
(for comparison 0.72 in LHCb)

$$(1) \cong |A_0|^2 \left[e^{-\Gamma_L t} \pm e^{-\Gamma_S t} \sin(\Delta m_s t) \times \varphi_s \times TP \times e^{-0.5(\sigma_t \Delta m_s)^2} \right] \times \\ \times 2 \cos^2 \psi_T (1 - \sin^2 \theta_T \cos^2 \phi_T)$$

$$(6) \cong |A_0| |A_\perp| \left[\frac{1}{2} (e^{-\Gamma_L t} - e^{-\Gamma_H t}) \cos \delta_{||} \times \varphi_s \pm e^{-\Gamma_S t} \cos(\delta_\perp - \Delta m_s t) \times TP \times e^{-0.5(\sigma_t \Delta m_s)^2} \right] \times \\ \times \frac{1}{\sqrt{2}} \sin 2\psi_T \sin^2 \theta_T \sin 2\phi_T$$

$$(9) \cong |A_S| |A_\perp| \sin(\delta_\perp - \delta_S) \left[e^{-\Gamma_H t} \mp e^{-\Gamma_S t} \sin(\Delta m_s t) \times \varphi_s \times TP \times e^{-0.5(\sigma_t \Delta m_s)^2} \right] \times \\ \times \frac{1}{3} \sqrt{6} \sin \psi_T \sin 2\theta_T \cos \phi_T$$

Combined likelihood fit



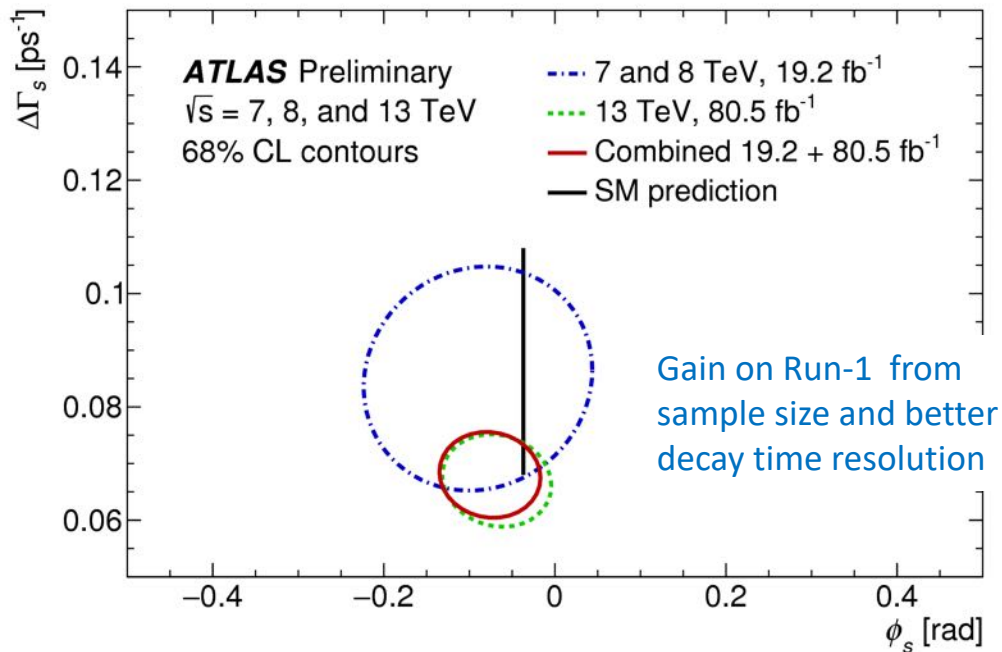
Fit projections

Unbinned likelihood fit on mass, decay time, angles, using per-event errors and fitting lifetimes, amplitudes, weak and strong phases.

Backgrounds: $B_d^0 \rightarrow J/\psi K^{*0}$ $\Lambda_b \rightarrow J/\psi p K^-$ $b\bar{b} \rightarrow J/\psi X$ $pp \rightarrow J/\psi X$

Main systematic uncertainty from tagging uncertainty

Fit results



Part-of-Run-2 results:

$$\varphi_s = -0.068 \pm 0.038 \pm 0.018$$

$$\Delta\Gamma_s = 0.067 \pm 0.005 \pm 0.002$$

[ATLAS-CONF-2019-009](#)

Combined ATLAS results
 Run-1 + part-of-Run-2
 (preliminary)

Parameter	Value	Statistical uncertainty	Systematic uncertainty
ϕ_s [rad]	-0.076	0.034	0.019
$\Delta\Gamma_s$ [ps ⁻¹]	0.068	0.004	0.003
Γ_s [ps ⁻¹]	0.669	0.001	0.001
$ A_{\parallel}(0) ^2$	0.220	0.002	0.002
$ A_0(0) ^2$	0.517	0.001	0.004
$ A_S ^2$	0.043	0.004	0.004
δ_{\perp} [rad]	3.075	0.096	0.091
δ_{\parallel} [rad]	3.295	0.079	0.202
$\delta_{\perp} - \delta_S$ [rad]	-0.216	0.037	0.010

Preliminary part-of-Run-2 result

	ϕ_s [rad]	$\Delta\Gamma_s$ [ps ⁻¹]	Γ_s [ps ⁻¹]	$ A_{\parallel}(0) ^2$	$ A_0(0) ^2$	$ A_S(0) ^2$	δ_{\perp} [rad]	δ_{\parallel} [rad]	$\delta_{\perp} - \delta_S$ [rad]
Tagging	1.7×10^{-2}	0.4×10^{-3}	0.3×10^{-3}	0.2×10^{-3}	0.2×10^{-3}	2.3×10^{-3}	1.9×10^{-2}	2.2×10^{-2}	2.2×10^{-3}
Acceptance	0.7×10^{-3}	$< 10^{-4}$	$< 10^{-4}$	0.8×10^{-3}	0.7×10^{-3}	2.4×10^{-3}	3.3×10^{-2}	1.4×10^{-2}	2.6×10^{-3}
ID alignment	0.7×10^{-3}	0.1×10^{-3}	0.5×10^{-3}	$< 10^{-4}$	$< 10^{-4}$	$< 10^{-4}$	1.0×10^{-2}	7.2×10^{-3}	$< 10^{-4}$
S-wave phase	0.2×10^{-3}	$< 10^{-4}$	$< 10^{-4}$	0.3×10^{-3}	$< 10^{-4}$	0.3×10^{-3}	1.1×10^{-2}	2.1×10^{-2}	8.3×10^{-3}
Background angles model:									
Choice of fit function	1.8×10^{-3}	0.8×10^{-3}	$< 10^{-4}$	1.4×10^{-3}	0.7×10^{-3}	0.2×10^{-3}	8.5×10^{-2}	1.9×10^{-1}	1.8×10^{-3}
Choice of p_T bins	1.3×10^{-3}	0.5×10^{-3}	$< 10^{-4}$	0.4×10^{-3}	0.5×10^{-3}	1.2×10^{-3}	1.5×10^{-3}	7.2×10^{-3}	1.0×10^{-3}
Choice of mass interval	0.4×10^{-3}	0.1×10^{-3}	0.1×10^{-3}	0.3×10^{-3}	0.3×10^{-3}	1.3×10^{-3}	4.4×10^{-3}	7.4×10^{-3}	2.3×10^{-3}
Dedicated backgrounds:									
B_d^0	2.3×10^{-3}	1.1×10^{-3}	$< 10^{-4}$	0.2×10^{-3}	3.1×10^{-3}	1.4×10^{-3}	1.0×10^{-2}	2.3×10^{-2}	2.1×10^{-3}
Λ_b	1.6×10^{-3}	0.4×10^{-3}	0.2×10^{-3}	0.5×10^{-3}	1.2×10^{-3}	1.8×10^{-3}	1.4×10^{-2}	2.9×10^{-2}	0.8×10^{-3}
Fit model:									
Time res. sig frac	1.4×10^{-3}	1.1×10^{-3}	$< 10^{-4}$	0.5×10^{-3}	0.6×10^{-3}	0.6×10^{-3}	1.2×10^{-2}	3.0×10^{-2}	0.4×10^{-3}
Time res. p_T bins	3.3×10^{-3}	1.4×10^{-3}	0.1×10^{-2}	$< 10^{-4}$	$< 10^{-4}$	0.5×10^{-3}	6.2×10^{-3}	5.2×10^{-3}	1.1×10^{-3}
Total	1.8×10^{-2}	0.2×10^{-2}	0.1×10^{-2}	0.2×10^{-2}	0.4×10^{-2}	0.4×10^{-2}	9.7×10^{-2}	2.0×10^{-1}	0.1×10^{-1}

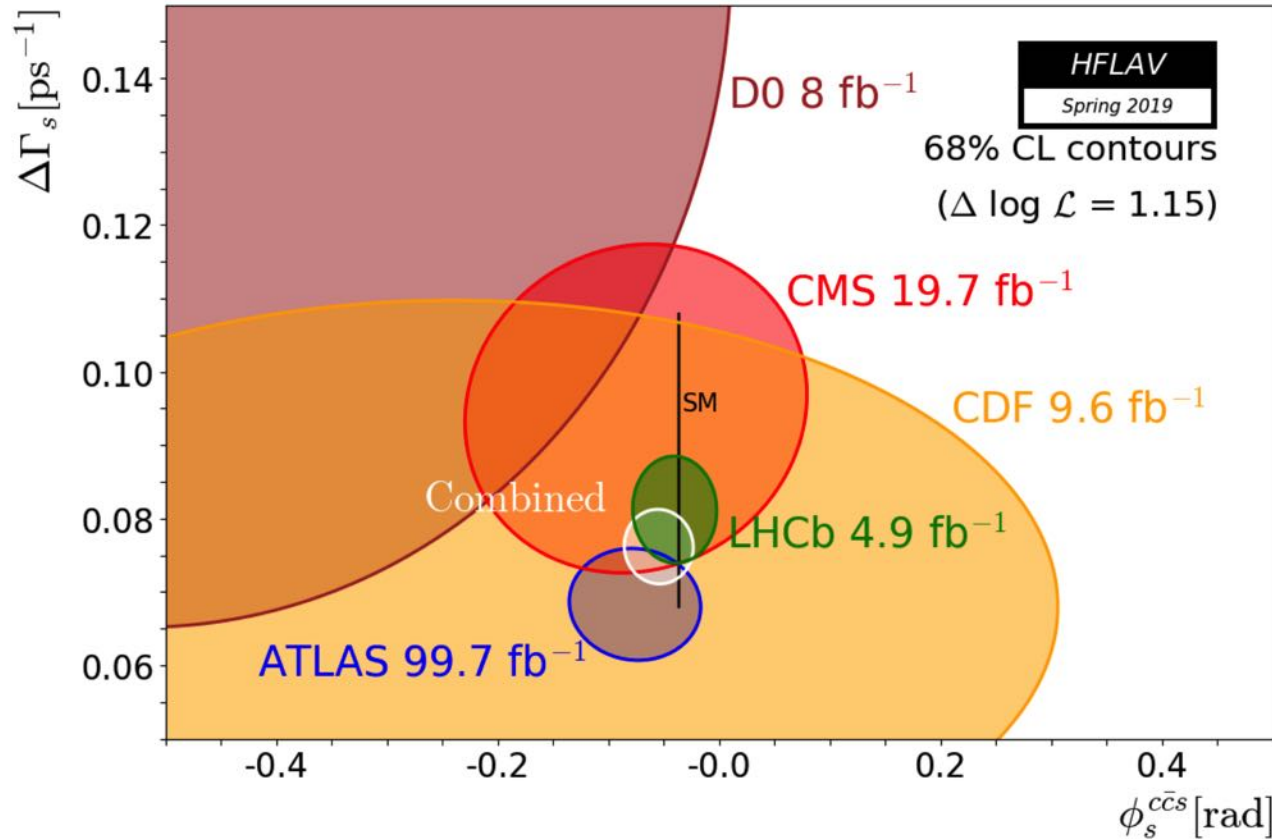
Statistical uncertainty 3.8×10^{-2} 0.5×10^{-2} 0.1×10^{-2} 0.2×10^{-2} 0.1×10^{-2} 0.3×10^{-2} 1.0×10^{-1} 8.2×10^{-2} 3.7×10^{-2}

Systematic uncertainties

Fit correlation matrix

	$\Delta\Gamma$	Γ_s	$ A_{\parallel}(0) ^2$	$ A_0(0) ^2$	$ A_S(0) ^2$	δ_{\parallel}	δ_{\perp}	$\delta_{\perp} - \delta_S$
ϕ_s	-0.111	0.038	0.000	-0.008	-0.015	0.019	-0.001	-0.011
$\Delta\Gamma$	1	-0.563	0.092	0.097	0.042	0.036	0.011	0.009
Γ_s		1	-0.139	-0.040	0.103	-0.105	-0.041	0.016
$ A_{\parallel}(0) ^2$			1	-0.349	-0.216	0.571	0.223	-0.035
$ A_0(0) ^2$				1	0.299	-0.129	-0.056	0.051
$ A_S(0) ^2$					1	-0.408	-0.175	0.164
δ_{\parallel}						1	0.392	-0.041
δ_{\perp}							1	0.052

Overall combination of measurements



Preliminary HFLAV combination:

$$\varphi_s = -0.055 \pm 0.021 \text{ rad}$$

$$\Delta\Gamma_s = 0.0764_{-0.0033}^{+0.0034} \text{ ps}^{-1}$$

LHCb combines measurements on $J/\psi K^+ K^-$ (non resonant) and $J/\psi \pi^+ \pi^-$ final states (Preliminary, Moriond-EW 2019)

ATLAS result compatible with SM, and with LHCb result (also updated in 2019)
 (Some tension on values of Γ_s , respectively about $+2/-2\sigma$ from previous world averages.)

Conclusions



ATLAS, and LHC in general, has achieved very significant results on B physics, aiming at evidence of new physics.

Deviations from the SM based predictions have not been found, while the allowed phase space of NP models has been reduced.

Large steps forward are expected from HL-LHC, which will complement the programme of Belle.

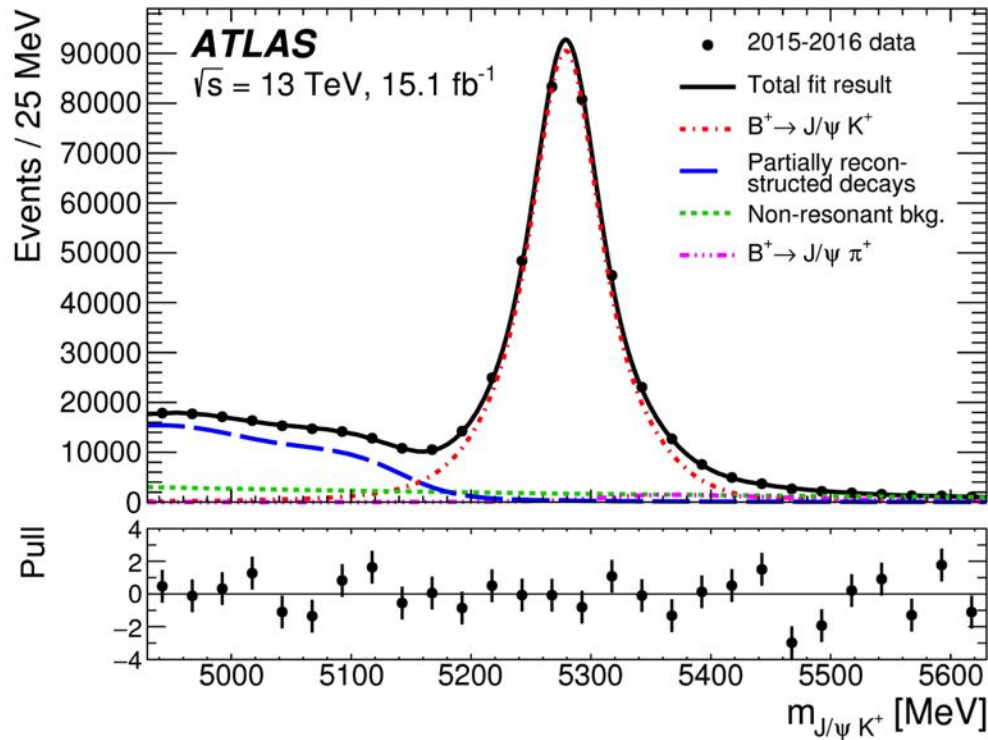
ADDITIONAL SLIDES

Rare decay:

Variable	Description
p_T^B	Magnitude of the B candidate transverse momentum \vec{p}_T^B .
$\chi_{PV,DV}^2$	Compatibility of the separation $\vec{\Delta x}$ between production (i.e. associated PV) and decay (DV) vertices in the transverse projection: $\vec{\Delta x}_T \cdot \Sigma_{\Delta x_T}^{-1} \cdot \vec{\Delta x}_T$, where $\Sigma_{\Delta x_T}$ is the covariance matrix.
ΔR_{flight}	Three-dimensional angular distance between \vec{p}^B and $\vec{\Delta x}$: $\sqrt{\alpha_{2D}^2 + (\Delta\eta)^2}$
$ \alpha_{2D} $	Absolute value of the angle in the transverse plane between \vec{p}_T^B and $\vec{\Delta x}_T$.
L_{xy}	Projection of $\vec{\Delta x}_T$ along the direction of \vec{p}_T^B : $(\vec{\Delta x}_T \cdot \vec{p}_T^B) / \vec{p}_T^B $.
IP_B^{3D}	Three-dimensional impact parameter of the B candidate to the associated PV.
$DOCA_{\mu\mu}$	Distance of closest approach (DOCA) of the two tracks forming the B candidate (three-dimensional).
$\Delta\phi_{\mu\mu}$	Azimuthal angle between the momenta of the two tracks forming the B candidate.
$ d_0 ^{\max\text{-sig.}}$	Significance of the larger absolute value of the impact parameters to the PV of the tracks forming the B candidate, in the transverse plane.
$ d_0 ^{\min\text{-sig.}}$	Significance of the smaller absolute value of the impact parameters to the PV of the tracks forming the B candidate, in the transverse plane.
p_L^{\min}	The smaller of the projected values of the muon momenta along \vec{p}_T^B .
$I_{0.7}$	Isolation variable defined as ratio of $ \vec{p}_T^B $ to the sum of $ \vec{p}_T^B $ and the transverse momenta of all additional tracks contained within a cone of size $\Delta R = \sqrt{(\Delta\phi)^2 + (\Delta\eta)^2} = 0.7$ around the B direction. Only tracks matched to the same PV as the B candidate are included in the sum.
$DOCA_{xtrk}$	DOCA of the closest additional track to the decay vertex of the B candidate. Only tracks matched to the same PV as the B candidate are considered.
N_{xtrk}^{close}	Number of additional tracks compatible with the decay vertex (DV) of the B candidate with $\ln(\chi_{xtrk,DV}^2) < 1$. Only tracks matched to the same PV as the B candidate are considered.
$\chi_{\mu,xPV}^2$	Minimum χ^2 for the compatibility of a muon in the B candidate with any PV reconstructed in the event.

Variables used in MVA classifier against continuum background

Rare decay:



Mass spectrum of B^+ candidates

Rare decay:

Source	Contribution [%]
Statistical	0.8
BDT input variables	3.2
Kaon tracking efficiency	1.5
Muon trigger and reconstruction	1.0
Kinematic reweighting (DDW)	0.8
Pile-up reweighting	0.6

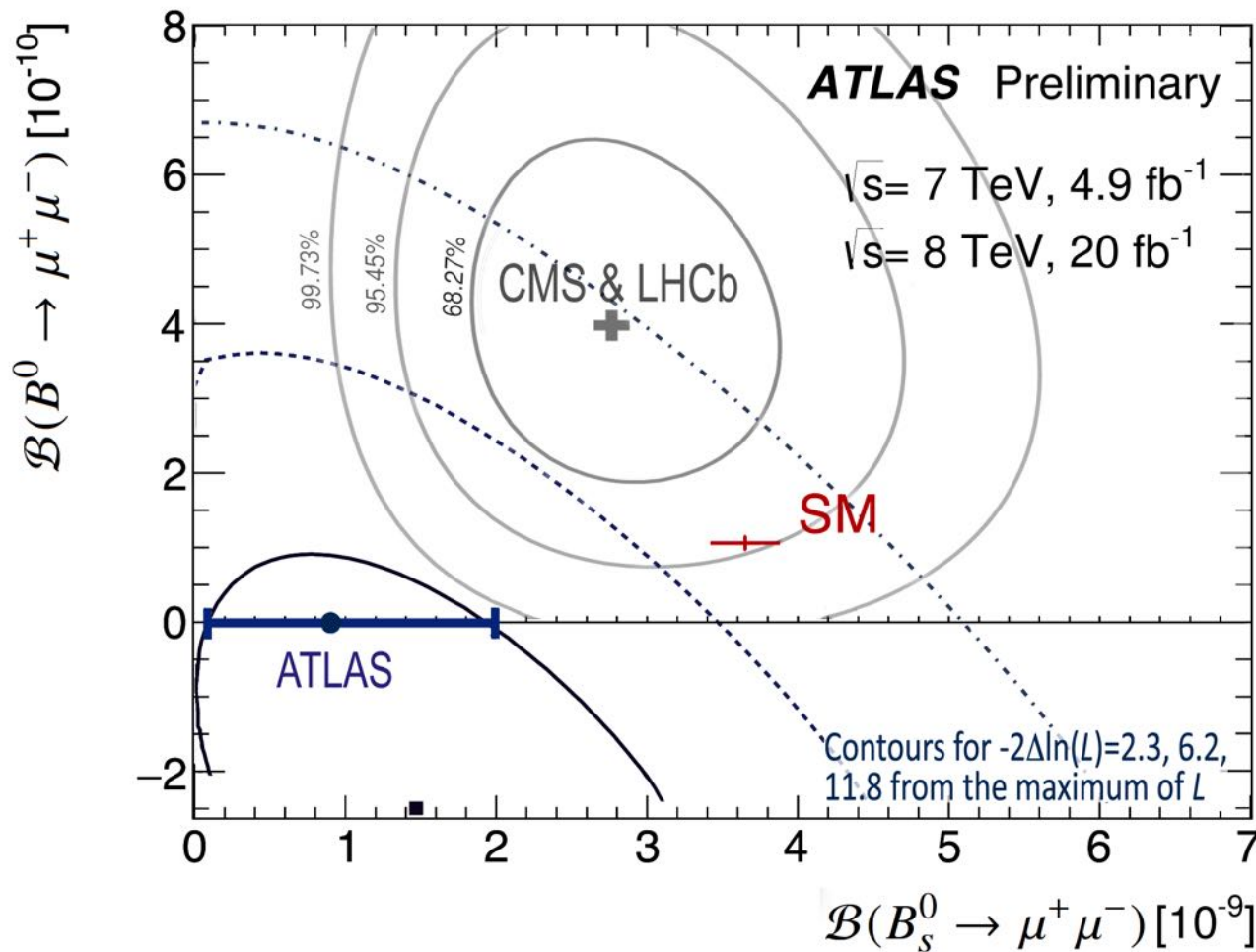
Systematic uncertainties on efficiency ratio ($B^+/B^0_{(s)}$)

Source	B_s^0 [%]	B^0 [%]
f_s/f_d	5.1	-
B^+ yield	4.8	4.8
$R_{\mathcal{E}}$	4.1	4.1
$\mathcal{B}(B^+ \rightarrow J/\psi K^+) \times \mathcal{B}(J/\psi \rightarrow \mu^+ \mu^-)$	2.9	2.9
Fit systematic uncertainties	8.7	65
Stat. uncertainty (from likelihood est.)	27	150

Systematic uncertainties on branching fractions

Rare decay: LHCb+CMS 2015 and ATLAS 2016

Likelihood contours



The contours corresponding to $-2\Delta\ln(L)=2.3, 6.2, 11.8$ are shown relative to the absolute maximum of L , regardless of its position outside of the natural boundary.

The minimum within the boundary of non-negative branching fraction is shown with the error bar for the frequentist 68% confidence range for $\text{BR}(B_s^0 \rightarrow \mu^+ \mu^-)$

Also shown are the contours from the combination of CMS and LHCb
 [Nature 522 (2015) 68-72]



φ_s : angular and time dependent amplitudes

k	$\mathcal{O}^{(k)}(t)$	$g^{(k)}(\theta_T, \psi_T, \phi_T)$
1	$\frac{1}{2} A_0(0) ^2 \left[(1 + \cos \phi_s) e^{-\Gamma_L^{(s)} t} + (1 - \cos \phi_s) e^{-\Gamma_H^{(s)} t} \pm 2e^{-\Gamma_s t} \sin(\Delta m_s t) \sin \phi_s \right]$	$2 \cos^2 \psi_T (1 - \sin^2 \theta_T \cos^2 \phi_T)$
2	$\frac{1}{2} A_{\parallel}(0) ^2 \left[(1 + \cos \phi_s) e^{-\Gamma_L^{(s)} t} + (1 - \cos \phi_s) e^{-\Gamma_H^{(s)} t} \pm 2e^{-\Gamma_s t} \sin(\Delta m_s t) \sin \phi_s \right]$	$\sin^2 \psi_T (1 - \sin^2 \theta_T \sin^2 \phi_T)$
3	$\frac{1}{2} A_{\perp}(0) ^2 \left[(1 - \cos \phi_s) e^{-\Gamma_L^{(s)} t} + (1 + \cos \phi_s) e^{-\Gamma_H^{(s)} t} \mp 2e^{-\Gamma_s t} \sin(\Delta m_s t) \sin \phi_s \right]$	$\sin^2 \psi_T \sin^2 \theta_T$
4	$\frac{1}{2} A_0(0) A_{\parallel}(0) \cos \delta_{\parallel} \left[(1 + \cos \phi_s) e^{-\Gamma_L^{(s)} t} + (1 - \cos \phi_s) e^{-\Gamma_H^{(s)} t} \pm 2e^{-\Gamma_s t} \sin(\Delta m_s t) \sin \phi_s \right]$	$\frac{1}{\sqrt{2}} \sin 2\psi_T \sin^2 \theta_T \sin 2\phi_T$
5	$ A_{\parallel}(0) A_{\perp}(0) \left[\frac{1}{2}(e^{-\Gamma_L^{(s)} t} - e^{-\Gamma_H^{(s)} t}) \cos(\delta_{\perp} - \delta_{\parallel}) \sin \phi_s \pm e^{-\Gamma_s t} (\sin(\delta_{\perp} - \delta_{\parallel}) \cos(\Delta m_s t) - \cos(\delta_{\perp} - \delta_{\parallel}) \cos \phi_s \sin(\Delta m_s t)) \right]$	$-\sin^2 \psi_T \sin 2\theta_T \sin \phi_T$
6	$ A_0(0) A_{\perp}(0) \left[\frac{1}{2}(e^{-\Gamma_L^{(s)} t} - e^{-\Gamma_H^{(s)} t}) \cos \delta_{\perp} \sin \phi_s \pm e^{-\Gamma_s t} (\sin \delta_{\perp} \cos(\Delta m_s t) - \cos \delta_{\perp} \cos \phi_s \sin(\Delta m_s t)) \right]$	$\frac{1}{\sqrt{2}} \sin 2\psi_T \sin 2\theta_T \cos \phi_T$
7	$\frac{1}{2} A_S(0) ^2 \left[(1 - \cos \phi_s) e^{-\Gamma_L^{(s)} t} + (1 + \cos \phi_s) e^{-\Gamma_H^{(s)} t} \mp 2e^{-\Gamma_s t} \sin(\Delta m_s t) \sin \phi_s \right]$	$\frac{2}{3} (1 - \sin^2 \theta_T \cos^2 \phi_T)$
8	$\alpha A_S(0) A_{\parallel}(0) \left[\frac{1}{2}(e^{-\Gamma_L^{(s)} t} - e^{-\Gamma_H^{(s)} t}) \sin(\delta_{\parallel} - \delta_S) \sin \phi_s \pm e^{-\Gamma_s t} (\cos(\delta_{\parallel} - \delta_S) \cos(\Delta m_s t) - \sin(\delta_{\parallel} - \delta_S) \cos \phi_s \sin(\Delta m_s t)) \right]$	$\frac{1}{3} \sqrt{6} \sin \psi_T \sin^2 \theta_T \sin 2\phi_T$
9	$\frac{1}{2} \alpha A_S(0) A_{\perp}(0) \sin(\delta_{\perp} - \delta_S) \left[(1 - \cos \phi_s) e^{-\Gamma_L^{(s)} t} + (1 + \cos \phi_s) e^{-\Gamma_H^{(s)} t} \mp 2e^{-\Gamma_s t} \sin(\Delta m_s t) \sin \phi_s \right]$	$\frac{1}{3} \sqrt{6} \sin \psi_T \sin 2\theta_T \cos \phi_T$
10	$\alpha A_0(0) A_S(0) \left[\frac{1}{2}(e^{-\Gamma_H^{(s)} t} - e^{-\Gamma_L^{(s)} t}) \sin \delta_S \sin \phi_s \pm e^{-\Gamma_s t} (\cos \delta_S \cos(\Delta m_s t) + \sin \delta_S \cos \phi_s \sin(\Delta m_s t)) \right]$	$\frac{4}{3} \sqrt{3} \cos \psi_T (1 - \sin^2 \theta_T \cos^2 \phi_T)$